

**Table S1. Nomenclature of Extracellular Vesicles and Nanoparticles**

Name	Category	EV class <sup>a</sup>	Size	Typical sedimentation	Protein markers	Biogenesis	Comments	Principal References
Classical exosome	Exosome	Small EV	40 - 150 nm	100,000 - 200,000 × g <sup>c</sup>	CD63, (CD81, CD9)	MVE	CD63 generally most accepted, CD81 and CD9 likely less specific but present. CD63 strongly labels MVEs <sup>h</sup>	Kowal et al 2016, van Niel et al 2018, this work
Non-classical exosome	Exosome	Small EV	40 - 150 nm	100,000 - 200,000 × g	? (CD63-, CD81- and CD9-negative)	MVE	Hypothetical CD63/CD81/CD9-negative exosome. Subpopulations of ILVs and MVEs may exist <sup>i</sup>	van Niel et al 2011, Edgar et al 2014, this work
Classical microvesicle	Microvesicle	Large EV	~ 150 - 1000 nm <sup>b</sup>	10,000 - 20,000 × g	Annexin A1, (ARF6, Annexin A2?)	Plasma membrane	This work identifies Annexin A1 as a marker of classical microvesicles	Muralidharan-Charivan et al 2009, this work
Large oncosome	Microvesicle	Large EV	1 - 10 μm	10,000 × g	Annexin A1, (ARF6, Annexin A2?)	Plasma membrane	This work identifies Annexin A1 as a likely marker of large oncosomes	Minciacci et al 2015, Miniciacci et al 2017, this work
ARMM	Microvesicle	Small EV	~ 40 - 100 nm	100,000 - 200,000 × g	ARRDC1, (TSG101) <sup>f</sup>	Plasma membrane	Small EV-sized budding microvesicles that depend on ARRDC1 and TSG101 for biogenesis	Nabhan et al 2012, Wang and Lu 2017, this work
Apoptotic body	Apoptotic EV	Large EV	1 - 5 μm	1,000 - 10,000 × g	Annexin V (PS exposure)	Apoptosis	Generally accepted size range for apoptotic bodies	Hristov et al 2004, Crescitelli et al 2013,
Apoptotic vesicle	Apoptotic EV	Small to large EV	~ 100 - 1000 nm	10,000 - 200,000 × g <sup>d</sup>	Annexin V (PS exposure)	Apoptosis	Apoptosis-related vesicle, this work demonstrates classical exosomes do not express Annexin V <sup>j</sup>	Hristov et al 2004, Schiller et al 2008, this work
Autophagic EV	Autophagic EV	Small to large EV	40 - 1000 nm?	10,000 - 200,000 × g <sup>e</sup>	LC3B-PE, p62	Autophagy	Does not express CD63, CD81 and CD9. extracellular release is induced by inhibition of autophagic flux	Hessvik et al 2016, this work
Exomere	Nanoparticle	Non-EV	~ 35 - 50 nm	100,000 - 200,000 × g	HSP90, HSPA13 <sup>g</sup>	Unknown	Perhaps represents composite/aggregation of secreted proteins and extracellular debris	Zhang et al 2018, Zhang et al 2019, this work
NV fractions	Nanoparticle	Non-EV	? (vaults: ~ 70 nm)	100,000 - 200,000 × g	Fibronectin, Histones, MVP, HSPA13 <sup>g</sup>	Unknown	Perhaps represents composite/aggregation of secreted proteins and extracellular debris including vaults	This work

EV, extracellular vesicle; sEV, small extracellular vesicle; MVE, multivesicular endosome; SIM, Structured Illumination Microscopy; ARMM, arrestin-domain-containing protein 1 (ARRDC1)-mediated microvesicle; PS, phosphatidylserine; NV, non-vesicular.

<sup>a</sup>The terms Small EV (<200 nm) and Large EV (>200 nm) for lipid bilayer-delimited extracellular vesicles (EVs) are somewhat arbitrary but widely adopted. In this work, samples were passed through a 220 nm pore filter before isolation of small EV samples.

<sup>b</sup>In this work, we observe Annexin A1-positive vesicles down to about 150 nm in size using SIM, which is at the resolution limit of reliable identification of a vesicle budding from the plasma membrane. Better resolution may allow <150 nm classical microvesicles to be observed.

<sup>c</sup>Significant sedimentation of exosomes/sEVs occurs already at 33,000 × g (Jeppesen et al 2014a). Differential ultracentrifugation will produce enrichment of specific EVs but is incapable of generating samples of purely one type of EV.

<sup>d</sup>Presumed, based on the size-range of vesicles bearing Annexin V.

<sup>e</sup>Presumed, based on the size-range of vesicles bearing LC3B-PE.

<sup>f</sup>In this work, we demonstrate that at least some ARRDC1-positive sEVs also express CD9 and CD81. In particular, CD9-positive sEVs from the Gli36 cell line strongly expressed ARRDC1. The expression of TSG101 was very low in CD63- and CD81-positive sEVs but robust in CD9-positive sEVs.

<sup>g</sup>HSP90 was associated with exomeres (Zhang et al 2018) and is absent from classical exosomes (this work). HSPA13 was associated with exomeres (Zhang et al 2018, Zhang et al 2019), and NV fractions (this work). Other heat shock proteins may be associated with exosomes or sEVs, including HSC70 (Kowal et al 2016, this work).

<sup>h</sup>In this work, we demonstrate that some CD63-positive organelles also stain for LC3B, indicative of amphisomes - the fusion products of MVEs and autophagosomes. However, CD63-positive exosomes do not express LC3B-PE.

<sup>i</sup>There is evidence for CD63-dependent and -independent ILVs (van Niel et al 2011), and for CD63-dependent and Hrs-dependent subpopulations of ILVs in the same MVEs (Edgar et al 2014). sEVs that are distinct from classical exosomes must be significant carriers of extracellular proteins previously associated with exosomes (this work), but these sEVs could be non-classical, MVE-derived, exosome.

<sup>j</sup>At least under conditions where apoptosis is not deliberately induced. In this work, we demonstrate that classical exosomes do express Annexin V, but Annexin V is present in gradient purified sEV fractions.

### Table S1. Nomenclature of Extracellular Vesicles and Nanoparticles, Related to Figures 1-7.

Nomenclature of terms used to describe extracellular vesicles and nanoparticles in the context of this study. Note that the term 'extracellular vesicles' refers exclusively to lipid bilayer-membrane enclosed vesicles and thus distinct from non-membrane enclosed nanoparticles such as exomeres and the NV fractions, and from lipoprotein complexes such as HDL.

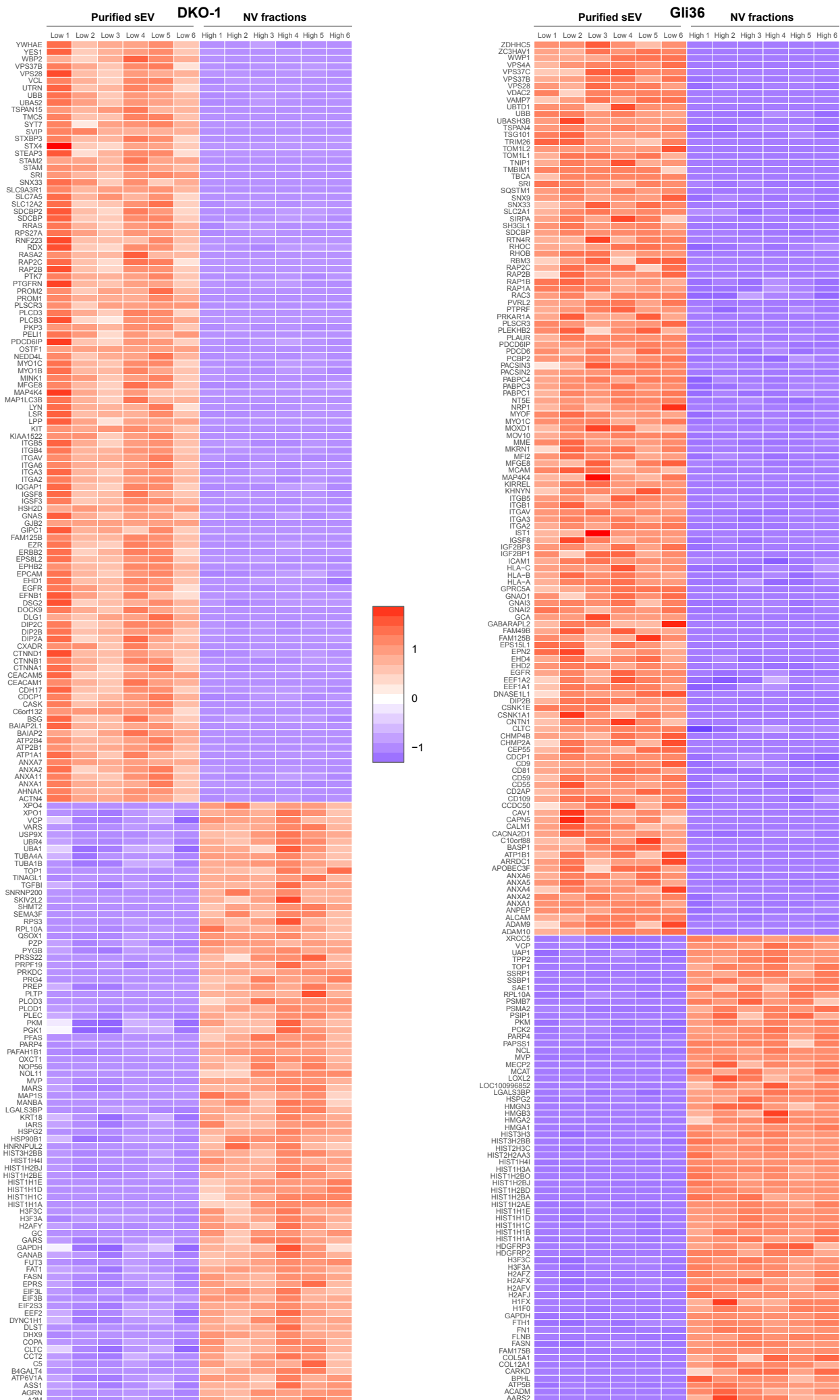


**Table S2. Top 200 proteins most significantly differentially expressed between purified sEV and non-vesicular (NV) fractions, Related to Figure 2.** Small EVs (low density) and non-vesicular (high density) fractions were separated by high-resolution density gradient centrifugation followed by proteomic analysis. Heat map scale indicates intensity, defined as  $\Delta(\text{spectral counts} - \text{mean spectral counts})/\text{standard deviation}$ .

DKO-1				Gli36	
Cell	Large EV	Small EV	Non-vesicular	Small EV	Non-vesicular
GAPDH	AHNAK	PDCD6P	PKM	CLTC	GAPDH
EEF2	GAPDH	PDCD6P	CLTC	PDCD6P	HIST1H4I
HSP90AA1	PKM	AHNAK	PKM	PDCD6P	MVP
HSP90AB1	ACTG1	SDCBP	PKM	GAPDH	PGK1
KRT18	PKM	SDCBP	DYNC1H1	NTSE	CLTC
KRT8	PKM	SDCBP	GAPDH	ANPEP	FTH1
EEF1A1	ANXA2	NTSE	MVP	SDCBP	PKM
FLNA	HSPG2	NTSE	FAT1	SDCBP	HSP90AB1
PKM	FLNA	ITGB4	FASN	HSPA8	PKM
AHNAK	FLNB	ITGB4	PGK1	EEF1A1	HIST1H4A
ACTG1	IQGAP1	DFP2B	HSPG2	UBB	FASN
ENO1	DYNC1H1	PKM	HSP90AA1	HSPA1A	VCP
PLEC	ENO1	GAPDH	EEF2	ENO1	FLNB
PLEC	CLTC	PKM	FLNB	PGK1	DYNC1H1
TUBB	EZR	CLTC	MYH9	HSP90AB1	FN1
PKM	AGRN	ITGA6	PRKDC	PABPC1	HIST2H3C
PKM	MYH9	PKM	HSP90AB1	EEF1A2	TUBB
HSPD1	MYO1C	ITGA6	UBR4	HLA-A	FLNA
TUBB4B	PSK1	ACTG1	AGRN	HSPA8	PCK2
FASN	ALDOA	PTGFRN	VCP	HSP90AA1	HSP90AA1
HSPA8	SPTAN1	CTNND1	PLEC	PKM	ATP5B
TUBB4A	HSP90AA1	EZR	PLEC	DYNC1H1	PARR4
TUBB2B	ACTN4	MYO1C	UBA1	ACTG1	H3F3A
CLTC	ITGB4	HSPA8	TUBB4B	MYO1C	TUBB4B
MYH9	SPTBN1	IQGAP1	ENO1	EH2	HIST2H2AA3
TUBA1B	ITGB4	DYNC1H1	TUBB	PABPC4	ACTG1
SPTAN1	ACTA1	MYOF	HIST1H4I	FTH1	HSP90B1
FLNB	CTNND1	CD81	TUBA1B	MOV10	EEF2
SPTBN1	SPTBN1	ENO1	EPRS	MIE	HIST1H2BD
DYNC1H1	HSP90AB1	SLC12A2	TGFB	PKM	UBA1
TUBA1C	MYO1B	ANXA2	KIAA1199	HLA-B	HSPA8
SPTBN1	MYO1B	PLXNB2	PARR4	CLTCL1	H2AFZ
NCL	ACTG2	PGK1	TUBA1C	ANXA8	H2AFJ
PRKDC	PLEC	ITGB1	ACTG1	ANXA2	PYGL
TUBB2A	PLEC	UBB	TUBB4A	TLN1	TUBB2A
TUBA4A	MYOF	ATP1A1	CLTCL1	TUBB	SERPINE1
EEF1A2	NTSE	RPS27A	TUBB2A	SGSTM1	TUBB4A
HIST1H4I	HSPA8	UBA52	TUBB2B	MYOF	HIST1H2BD
ALDOA	MYO1D	FLNB	PDCD6P	TUBA1B	VIM
HSP90B1	ITGA6	ITGAV	LGALS3BP	MF12	HSPA8
VCP	ITGA6	CTNND1	PDCD6P	FLNA	NAMPT
XRCC5	PLXNB2	MYO1D	GANAB	EGFR	H2AFY
HNRNP1	YWHAZ	HSP90AA1	TUBA4A	SH3GL1	HIST1H2AE
LRPPRC	NTSE	ITGA3	HSPA8	CACNA2D1	TOP1
HSPA5	POTEE	HSPA1A	GANAB	SLC3A2	H2AFY
HNRNP1	FASN	MFG8	CCT2	ITGB1	TUBA1B
UBA1	LDHA	ADAM10	HSP90B1	TUBA1C	MYH9
CCT2	EEF1A1	CTHFP1	IRS	HSP90B1	HIST1H3
ANXA2	EEF2	IGSF8	HIST1H2BE	DDA1	ENO1
ACTN4	ITGB1	CASK	QSOX1	ANXA5	H2AFV
EPRS	ATP1A1	EPCAM	FLNA	LDHA	HSPA1A
ACTA1	PDCD6P	CD9	LDHA	TUBB4B	HSPG2
GANAB	PDCD6P	CTNNA1	XPO1	EEF2	HIST1H2BJ
XRCC6	CTNNA1	ALDOA	HIST1H2BJ	IGSF8	TUBA1C
GANAB	TUBB	SLC2A1	TUBB3	DIF2B	LGALS3BP
LDHB	EPCAM	MYO1B	WDR1	KRT1	GARS
HNRNP2B1	RDX	FAT1	KRT18	ITGAV	H2AFX
TUBA8	HSPA5	MYO1B	PKG2	ICAM1	H3F3C
KRT19	TUBB4B	PDCD6P	ALDOA	SNX33	TUBB6
GCN1L1	VCP	HSP90AB1	GFP11	TUBA4A	XRCC6
HNRNP1	SLC2A1	JUP	PYGL	HSPA1L	HIST1H1D
LDHA	HIST1H4I	EPH2	CAND1	PTPRF	HIST1H1C
LMNA	TPH1	GNAI2	COPA	EH2	EPRS
P4HB	CTNND1	ITGA2	HIST1H2BB	TUBB2A	HIST1H1E
CCT4	KRT8	TLN1	KPNB1	PABPC3	TLN1
TUBB6	UBA1	ACTA1	DPYSL2	FLNB	TUBA4A
RPL3	UTRN	FLNA	ASB1	UBA1	TUBB3
NPM1	TLN1	LDHA	HSPA5	TUBB4A	XRCC6
RPL4	ACTG2	SLC3A2	TLN1	TPH1	H1FO
HNRNP1	FAM128B	ATP2B1	KRT8	CDCP1	ACTC1
ACTG2	GPI	RDX	PGM1	VPS37B	FLNC
LMNA	ACTBL2	NCKAP1	IPO7	HSPA2	GANAB
TUBA3E	KRT18	GNAI3	RNPEP	FASN	OAT
HIST1H2BE	JUP	UTRN	PSMD2	ACTC1	FSCN1
PDIA3	ACTN1	YWHAZ	CCT8	KRT10	ATC
HSPA9	EPH2	FASN	ACYL	TSG1D1	HIST2H2AB
YWHAZ	MYH14	EEF1A1	NAMPT	FSCN1	ACTG2
EZR	CFL1	PKP3	MYH14	EH2	CS
EIF3A	GNAI3	CDCP1	SNRNP200	VIM	ALDH1A3
TPH1	ITGAV	MYH9	HSPA1A	HLA-C	EEF1A1
TUBB3	GNAI2	RAP1B	TUBA8	MSN	MPEP
POTEE	TUBA1B	EGFR	CRZ	CD2AP	NDRG1
SNRNP200	TUBB2B	POTEE	LDHA	HIST1H4I	HYOU1
TLN1	GFP11	NEDD4L	EP3L	MYH9	BANF1
PGK1	TUBB4A	CD55	VAR5	CD81	HSPA9
DSF	POTEE	ACTN4	CCT4	HLA-C	HIST1H1B
SYNCRP	VCL	MRK1	TUBA3E	SNY9	PDCD6P
NPM1	ANXA1	ACTG2	PGM1	ADAM10	AARS
CFL1	SFN	TPH1	PRSS23	CFL1	UAP1
CCT6A	LDHA	VCP	GARS	ANXA11	FTL
HSPA4	HSPA1A	AP2B1	ERO1L	VCP	PDCD6P
IPO5	TUBB2A	PTK7	CSE1L	VPS28	HIST1H2BB
HIST1H2AM	HSP90B1	LLGL2	PLOD1	ALDOA	PXDN
HSPH1	TUBA1C	IGSF3	XRCC6	CD55	TUBA3E
HIST1H3A	WDR1	UBA1	ACTA1	PTGFRN	IARS
IPO7	CSF1	PTK7	USP9X	PO2	PLEC
HIST2H2AC	CAND1	EH2	CCT8	KRT2	PYGB
HMGB1	POTEE	RAP1A	HUWE1	CD59	CLTCL1
VCL	ANXA5	FAM129B	EEF1A1	MFG8	HSPA4
CALR	MYO6	SDCBP2	SDCBP	PYGL	SBBP1

**Table S5. Top 100 most abundant proteins identified in cells, large EV and high-resolution density gradient purified sEV and non-vesicular fractions, Related to Figure 2.**

Proteomic analysis of DKO-1 cells, large EVs, small EVs and non-vesicular fractions (left), and Gli36 small EVs and non-vesicular fractions (right). Small EVs and non-vesicular fractions were separated by high-resolution density gradient fractionation. Proteins are ranked from top to bottom based on the number of spectral counts.



